

# Orientation of specifically $^{13}\text{C}=\text{O}$ labeled phosphatidylcholine multilayers from polarized attenuated total reflection FT-IR spectroscopy

Wigand Hübner and Henry H. Mantsch

Steele Institute for Molecular Sciences, National Research Council of Canada, Ottawa, Ontario, K1A 0R6, Canada

**ABSTRACT** Oriented multilayers of 1-myristoyl-2(1- $^{13}\text{C}$ )-myristoyl-*sn*-glycero-3-phosphatidylcholine (2[1- $^{13}\text{C}$ ]DMPC) and 1-palmitoyl-2(1- $^{13}\text{C}$ )-palmitoyl-*sn*-glycero-3-phosphatidylcholine (2[1- $^{13}\text{C}$ ]DPPC) were investigated by use of attenuated total reflection infrared spectroscopy with polarized light. Experiments were performed with the aim to determine the orientation of the two ester groups in these phospholipids in the solid state and in the hydrated state at temperatures below and above the respective gel to liquid-crystalline phase transitions. Substitution of the naturally occurring  $^{12}\text{C}$  carbonyl carbon atom by  $^{13}\text{C}$  in the ester group of the *sn*-2 chain of DMPC and DPPC shifts the infrared absorption of the carbonyl double bond stretching vibration to lower frequency. This results in two well-resolved ester  $\text{C}=\text{O}$  bands which can be assigned unequivocally to the *sn*-1 and *sn*-2 chains as they are separated by more than  $40\text{ cm}^{-1}$ . The two ester  $\text{CO}-\text{O}$  single bond stretching vibrations of the molecular fragments  $-\text{CH}_2\text{CO}-\text{OC}-$  are also affected and the corresponding infrared absorption band shifts by  $20\text{ cm}^{-1}$  on  $^{13}\text{C}$ -labeling of the carbonyl carbon atom. From the dichroic ratios of the individual ester bands in 2(1- $^{13}\text{C}$ )DMPC and 2(1- $^{13}\text{C}$ )DPPC we were able to demonstrate that the *sn*-1 and *sn*-2 ester  $\text{C}=\text{O}$  groups are similarly oriented with respect to the bilayer plane, with an angle  $\geq 60^\circ$  relative to the bilayer normal. The two  $\text{CO}-\text{O}$  single bonds on the other hand have very different orientations. The  $\text{CH}_2\text{CO}-\text{OC}$  fragment of the *sn*-1 chain is oriented along the direction of the all-*trans* methylene chain, whereas the same molecular segment of the *sn*-2 carbon chain is directed toward the bilayer plane. This orientation of the ester groups is retained in the liquid-crystalline phase. The tilt angle of the hydrocarbon all-*trans* chains, relative to the membrane normal, is  $25^\circ$  in the solid state of DMPC and DPPC multibilayers. In the hydrated gel state this angle varies between  $26^\circ$  and  $30^\circ$ , depending on temperature. Neither the orientation of the phosphate group, nor that of the choline group varies significantly in the different physical states of these phospholipids.

## INTRODUCTION

The bilayer structure of biological membranes is primarily a consequence of the amphiphilic nature of their constituent lipid molecules. Hence, a prerequisite for understanding the functional properties of complex membrane lipids, is a detailed knowledge of their preferred molecular conformations. A great deal of effort has been devoted during the last two decades to the problem of phospholipid conformation. Most of the work was carried out with phosphatidylcholines (PC) and phosphatidylethanolamines (PE) which constitute the major portion of mammalian membrane phospholipids.

Much of what is known today about lipid conformation is based on the x-ray single crystal structures of dimyristoyl PC (DMPC) and dilauroyl PE (DLPE) (1, 2). These early studies provide a picture of these lipid molecules with the glycerol moiety perpendicular to the bilayer plane and a fully extended all-*trans* acyl chain connected to the *sn*-1 glycerol carbon, whereas the first

segment of the *sn*-2 chain is oriented along the membrane plane until a  $90^\circ$  bend allows both chains to orient parallel to each other. From neutron diffraction experiments of specifically deuterium-labeled phospholipids it was concluded that this molecular arrangement also exists in the hydrated state of the bilayer (3-5) and  $^2\text{H}$ -NMR studies of phosphatidylcholines in the liquid-crystalline state further demonstrated a conformational nonequivalence of the first segments of the *sn*-1 and *sn*-2 acyl chains (6, 7). A theoretical interpretation, based on these experimental data, favored conformations near the glycerol moiety, similar to those found in the single crystal structure of DMPC (8).

On the other hand,  $^{13}\text{C}$ -NMR spectra of aqueous dipalmitoyl PC (DPPC) liposomes, specifically  $^{13}\text{C}$  enriched at the carbonyl position of the *sn*-2 chain, showed a drastic change in the orientation of the carbonyl-shielding tensor at the gel to liquid-crystalline phase transition temperature (9). After the molecular orientation of the ester chemical shielding tensor was established in 1986 (10), a subsequent  $^{13}\text{C}$ -NMR investigation of macroscopically aligned egg yolk phosphatidylcholine

Dr. Hübner's permanent address is Department of Physical Chemistry, University of Freiburg, D-7800 Freiburg, FRG.

in the liquid-crystalline state (11), and the study with DPPC liposomes (9), were interpreted as indicating that the *sn*-2 carbonyl bond direction is close to that of the magic angle (54.7°) whereas the *sn*-1 carbonyl bond direction is approximately perpendicular to the rotation axis of the lipid chains (or the bilayer normal). Such an orientation of the *sn*-2 carbonyl group, however, differs from the values of 61° and 80° obtained from the two lipid molecules in the unit cell of crystalline DMPC dihydrate (see Discussion in reference 9).

A singular structural picture of phospholipids in bilayers had to be reconsidered when the x-ray structure of dilauroyl phosphatidic acid revealed a reversed alignment of the initial segments of the two acyl chains (12), namely a 90° bend next to the C<sub>2</sub> atom of the *sn*-1 chain, and a fully extended all-*trans sn*-2 chain, starting from the C<sub>2</sub>-glycerol backbone. Based on the available information for x-ray structures of different phospholipids, and on <sup>1</sup>H-NMR investigations of phospholipids in the micellar and monomeric state, Hauser et al. (12) proposed a general model for phospholipids in the liquid-crystalline state. In the Hauser model, the x-ray structures of four different lipids (representing minimum energy potentials), can interconvert rapidly by conformational changes in torsion angles of the glycerol backbone and of the initial segments of the two acyl chains that contain the two carbonyl ester groups. Two out of the four interconversions allow an exchange of the bend conformation between the *sn*-1 and *sn*-2 chain. This model for bilayers in the liquid-crystalline state is certainly very interesting and should be scrutinized by different experimental techniques.

Polarized infrared spectroscopy has proven in the past to be a powerful tool for the determination of the orientation and conformation of specific segments within macroscopically aligned bilayers in the solid (13, 14) and the hydrated state (15–17). Unfortunately, most of these investigations could not assign separate vibrational bands to the *sn*-1 and *sn*-2 chain, a prerequisite for the assessment of conformational and orientational differences near the glycerol backbone. Therefore, we have turned to phospholipids with specifically <sup>13</sup>C labeled ester carbonyl groups. Herein we describe an attenuated total reflection (ATR) FT-IR polarization study with oriented multilayers of 2(1-<sup>13</sup>C)DMPC and 2(1-<sup>13</sup>C)DPPC in the solid state, in the gel state, and in the liquid-crystalline state. The two most important vibrational modes of the ester group in diacyl lipids, the C=O double bond stretching vibration and the CO—O single bond stretching vibration, can thus be assigned unambiguously to the unlabeled *sn*-1 chain and the <sup>13</sup>C labeled *sn*-2 chain in DMPC and DPPC.

## MATERIALS AND METHODS

The <sup>13</sup>C=O labeled lipids 2(1-<sup>13</sup>C)DMPC and 2(1-<sup>13</sup>C)DPPC were synthesized according to the procedure of Mason et al. (18). The starting fatty acids (1-<sup>13</sup>C) myristic acid and (1-<sup>13</sup>C) palmitic acid (MSD isotopes; Merck, Sharp & Dohme, Canada) were 99% <sup>13</sup>C enriched in the carboxyl carbon atom. Isomeric chain impurities of the synthesized lipids, caused by chain migration during the recylation step of the lyso-PCs, were <3% as checked by <sup>13</sup>C-NMR. Methyl (1-<sup>13</sup>C) palmitate was synthesized and purified from (1-<sup>13</sup>C) palmitic acid and methanol/borotrifluoride by use of standard procedures. Methyl palmitate was purchased from Nu-Chek Prep. Inc. (Elysian, MN).

Infrared spectra were recorded with a Digilab (Cambridge, MA) Fourier transform spectrometer (model FTS-60) equipped with a liquid nitrogen cooled mercury cadmium telluride detector. Transmission spectra of methyl palmitate as CCl<sub>4</sub> solutions (*c* = 10 mg/ml) were measured in a sealed liquid cell (100 μm) with NaCl windows. For polarized ATR measurements we used an overhead ATR unit (model 2FM; Wilmad Glass Co., Buena, NJ) and a parallelogram-shaped germanium ATR crystal (50 × 20 × 2 mm, face angle  $\theta$ :45°). A grid polarizer on KRS5 (Cambridge Optics, Cambridge, MA) was placed behind the ATR unit, the settings for parallel and perpendicular polarized light were under the control of the spectrometer computer. The upper side of the horizontally aligned ATR plate was covered with a home-built steel cell and sealed by means of a rubber O-ring, creating a sample compartment with a volume of ~500 μl. The temperature inside the sample compartment was regulated by flowing a thermostatically controlled glycol/water mixture through the cell. Oriented films were prepared by spreading a stock solution of lipid in chloroform (*c* = 5–7 mg/ml) on one side of the germanium plate. Uniform film homogeneity was achieved by slowly moving the solution with a Teflon bar along the crystal until complete evaporation of the solvent. By use of this method, a film thickness between 2.5–4 μm was obtained, which is much greater than the penetration depth of the evanescent wave (0.2–0.8 μm in the frequency range 4,000–1,000 cm<sup>-1</sup> for germanium with  $\theta$  = 45°). The steel cell, equipped with two inlets into the sample compartment, was then mounted on top of the film-covered side of the germanium crystal. Infrared spectra of the solid films were recorded with parallel and perpendicular polarized light. Typically, 500 scans were recorded with a resolution of 2 cm<sup>-1</sup>. Parallel and perpendicular polarized spectra of the blank germanium plate (with the mounted sample chamber), were used as single beam references.

To hydrate the film, the sample compartment was carefully filled with H<sub>2</sub>O through one of the two inlets of the cell. A copper constantan thermocouple was introduced through the second inlet to monitor the temperature in the aqueous phase. Subsequently, the temperature was slowly decreased to the desired starting temperature, and after an equilibration time of several hours, polarization measurements were performed as a function of increasing temperature. The temperature was increased in small steps (2°C) and the sample allowed to equilibrate for at least 30 min at a given temperature, before each measurement. This procedure was entirely under the control of the spectrometer computer. The lipid bilayers tend to swell with increasing temperature in the gel phase, and especially at the phase-transition temperature, which leads to a decrease of the total infrared absorbance. This process is reversible upon decreasing the temperature. Therefore, we always recorded a total of four spectra at a given temperature, alternating the parallel and perpendicular polarizations. Only if the first and third spectrum, recorded with parallel polarized light (and the second and fourth spectrum, recorded with perpendicular polarized light) were identical in intensity, did we calculate the

dichroic ratios by using the first and second (or the third and fourth) spectra.

After a completed heating cycle the sample was cooled to 10°C, equilibrated for 1 h after which the aqueous supernatant was removed with two syringes (fitted in the two inlets) without dismantling the cell. The wet lipid film was subsequently dried by gently blowing a stream of dry nitrogen through the sample compartment. Dichroic ratios from spectra of this dry film, acquired from the aqueous phase, were indistinguishable from those of the first dry film, acquired from the chloroform phase. To study hydrated films in the spectral region 1,600–1,800 cm<sup>-1</sup> which contains a strong band due to H<sub>2</sub>O, we rehydrated the dry lipid film with D<sub>2</sub>O and proceeded as described above. Solid films of methyl palmitate were prepared by evaporation from a hexane solution (*c* = 10 mg/ml).

Dichroic ratios of infrared bands were obtained by ratioing the integrated intensities of the absorbance bands obtained with parallel and perpendicular polarized light. In some cases it was necessary to use a band simulation program to obtain the integrated intensity of overlapping bands. The formula for calculating the order parameter *f* and the angle *B* from the dichroic ratio *R* are given in the Appendix, along with an error estimation.

## RESULTS

### Infrared spectra of methyl palmitate and methyl (1-<sup>13</sup>C)palmitate

Methyl palmitate and its <sup>13</sup>C=O labeled isomer were chosen to help assign the infrared vibrations that originate from the ester carbonyl groups. Fig. 1 shows IR transmission spectra of the two esters dissolved in CCl<sub>4</sub>. The most prominent difference between the two spectra in the spectral region between 1,100 and 1,800 cm<sup>-1</sup> is a shift in frequency of the C=O stretching band by 42 cm<sup>-1</sup> (from 1,742 to 1,700 cm<sup>-1</sup>), and a shift by 20 cm<sup>-1</sup> of the CO—O stretching band (from 1,172 to 1,152 cm<sup>-1</sup>) on substitution of <sup>12</sup>C=O by <sup>13</sup>C=O. The calculated isotope effect for an isolated C=O double bond vibration is 40 cm<sup>-1</sup>, which is close to the experimentally

observed shift. Jones (19) first noticed that the spectra of long chain fatty acid methyl esters (dissolved in CCl<sub>4</sub>) are very similar and a complete assignment of all vibrational bands was established for methyl laurate (20). Based on this investigation, the infrared bands in Fig. 1 at 1,172, 1,197, and ~1,250 cm<sup>-1</sup> can be related to a “zone vibration” involving the CH<sub>2</sub>CO—O fragment, whereby the skeletal CO—O single bond vibration is coupled with the αCH<sub>2</sub> deformation mode. Isotopic labeling results only in a minor shift in frequency of the two high frequency component bands, but leads to a 20-cm<sup>-1</sup> shift of the component band at 1,172 cm<sup>-1</sup>, therefore this band of the “zone vibration” can be regarded as the principal CO—O single bond vibration.

To assign the frequencies of the ester carbon-oxygen single and double bonds of methyl palmitate and methyl (1-<sup>13</sup>C)palmitate in the solid state, we examined both compounds deposited as films on an ATR plate. Infrared spectra of oriented multilayers are shown in Fig. 2. The most obvious difference between the two spectra is a shift in frequency of the C=O double bond vibration from 1,740 to 1,698 cm<sup>-1</sup>, along with a shift of the CO—O single bond vibration from 1,177 to 1,158 cm<sup>-1</sup> on labeling the carbonyl group with a <sup>13</sup>C atom. The other two frequency components of the “zone vibration” are no longer visible because of decreased intensity and/or overlap with the CH<sub>2</sub> wagging band progression of the ordered all-*trans* methylene chains. These well known, nearly equally spaced CH<sub>2</sub> wagging bands (at 1198, 1219, 1242, 1265, 1287, 1310, and 1330 cm<sup>-1</sup>), are only slightly affected by the isotopic exchange of <sup>12</sup>C=O with <sup>13</sup>C=O, resulting in a low-frequency shift of the individual component bands by 1–2 wavenumbers.

By comparing the infrared spectrum of the ester in the solid state (all-*trans* arrangement of the methylene groups along the direction of the acyl chains), with that

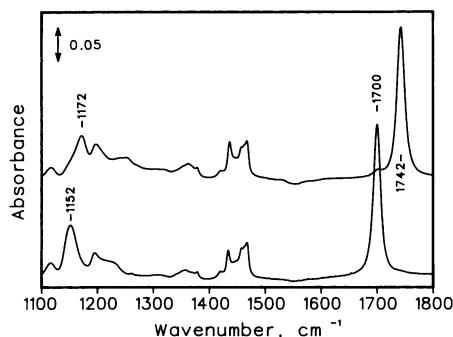


FIGURE 1 Transmission FT-IR spectra of methyl (1-<sup>13</sup>C) palmitate (bottom) and methyl (1-<sup>12</sup>C) palmitate (top) as solutions in CCl<sub>4</sub>. The C=O double bond (right) and CO—O single bond (left) vibrations are indicated by their respective frequencies.

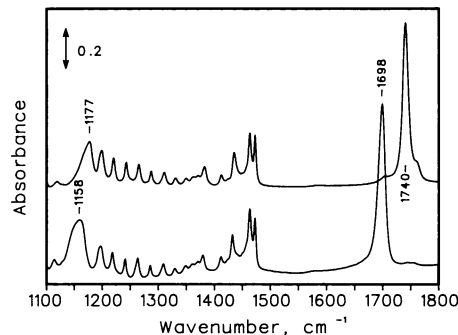


FIGURE 2 ATR-FT-IR spectra of crystalline methyl (1-<sup>13</sup>C) palmitate (bottom) and methyl (1-<sup>12</sup>C) palmitate (top). The ester C=O double bond and CO—O single bond vibrations are indicated by their respective frequencies.

of the highly disordered state of the ester in  $\text{CCl}_4$  solution, one finds only a small increase in the frequency of the double bond vibration, i.e., from 1,740 to 1,742  $\text{cm}^{-1}$  for  $^{12}\text{C}=\text{O}$ , and from 1,698 to 1,700  $\text{cm}^{-1}$  for  $^{13}\text{C}=\text{O}$ . At the same time, the  $\text{CO}-\text{O}$  single bond vibration decreases by  $\sim 5 \text{ cm}^{-1}$ , i.e., from 1,177 to 1,172  $\text{cm}^{-1}$  for  $^{12}\text{CO}-\text{O}$ , and from 1,158 to 1,152  $\text{cm}^{-1}$  for  $^{13}\text{CO}-\text{O}$ .

The next step was to estimate the direction of the transition moment of the ester  $\text{CO}-\text{O}$  single bond stretching vibration in the oriented film. The polarized ATR-FT-IR spectra of solid methyl palmitate are shown in Fig. 3. The seven absorption bands of the  $\text{CH}_2$  wagging band progression (transition moment along the direction of the all-*trans* methylene chain) exhibit a very high dichroic ratio of  $R^{\text{ATR}} \geq 30$ . The dichroic ratio  $R$  is defined as the intensity ratio of an absorbance band recorded with parallel polarized infrared light and the band recorded with perpendicular polarized light (see Appendix). The high  $z$ -polarization indicates that the acyl chains are oriented perpendicular to the  $xy$ -plane of the ATR crystal. The transition moments obtained for the alkyl  $\text{CH}_3$  and methoxy  $\text{CH}_3$  symmetric deformation bands at 1,435 and 1,382  $\text{cm}^{-1}$ , respectively, are also  $z$ -polarized. The  $xy$ -polarization of the  $\delta\text{CH}_2$  scissoring bands at 1,462 and 1,472  $\text{cm}^{-1}$  and that of the  $\alpha\text{CH}_2$  scissoring band at 1,410  $\text{cm}^{-1}$  ( $R^{\text{ATR}} \leq 1$ ) confirm the perpendicular orientation of the all-*trans* alkyl chains relative to the crystal surface, as the transition moments of these vibrational modes are located in the plane spanned by the two  $\text{C}-\text{H}$  bonds of the  $\text{CH}_2$  groups. The  $\text{CO}-\text{O}$  single bond vibration at 1,177  $\text{cm}^{-1}$  is also highly  $z$ -polarized ( $R^{\text{ATR}} \geq 25$ ); hence, the transition moment of this vibration must be oriented along the direction of the all-*trans* methylene chains (or perpendicular to the  $xy$ -plane of the ATR crystal). The same behavior was

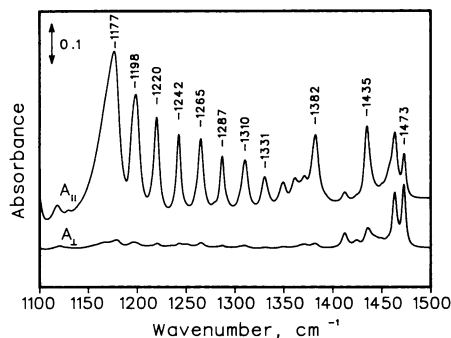


FIGURE 3 Polarized ATR-FT-IR spectra of macroscopically oriented methyl palmitate multilayers. The top spectrum was recorded with parallel polarized light ( $A_{||}$ ), and the bottom spectrum with perpendicular polarized light ( $A_{\perp}$ ) relative to the plane of incidence.

observed for the  $^{13}\text{CO}-\text{O}$  single bond vibration at 1,158  $\text{cm}^{-1}$  of methyl ( $^{13}\text{C}$ )palmitate. From polarized IR measurements of highly oriented polyester chains, Bradbury et al. (21) also proposed that the transition moment for the  $\text{CO}-\text{O}$  single bond vibration at 1,170  $\text{cm}^{-1}$  lies in the  $\text{C}_1(\text{C}_2=\text{O})\text{O}_2$  plane, with the direction of the transition moment pointing from  $\text{C}_1$  to  $\text{O}_2$ . The transition moment of the carbonyl bond is oriented along the  $\text{C}=\text{O}$  bond direction (22).

### Oriented films of 2( $^{13}\text{C}$ )DMPC and 2( $^{13}\text{C}$ )DPPC on a germanium substrate

We now apply the infrared spectroscopic information obtained from the above model esters to oriented films of 2( $^{13}\text{C}$ )DMPC and 2( $^{13}\text{C}$ )DPPC. As an example, Fig. 4 illustrates spectra of 2( $^{13}\text{C}$ )DPPC multilayers on a germanium ATR crystal, recorded with parallel ( $A_{||}$ ) and perpendicular ( $A_{\perp}$ ) polarized light. The top trace in Fig. 4 shows the difference spectrum  $A_{||} - A_{\perp}$ . The assignments of the most relevant infrared bands in oriented solid films of 2( $^{13}\text{C}$ )DMPC and 2( $^{13}\text{C}$ )DPPC are listed in Table 1, together with their dichroic ratio  $R$  ( $R = A_{||}/A_{\perp}$ ), the calculated order parameters  $f$  and the angles  $\beta$ . The angle  $\beta$  denotes the direction of the transition moment of a given infrared vibration relative to the bilayer normal (or the  $z$ -axis of the ATR crystal). The procedure of calculating  $f$  and  $\beta$  from the experimentally derived dichroic ratios  $R$ , is outlined in the Appendix. From the  $R$  values of the symmetric  $\text{CH}_2$  stretching band at 2,850  $\text{cm}^{-1}$ , the  $\delta\text{CH}_2$  bending bands at 1,467  $\text{cm}^{-1}$  and the  $\text{CH}_2$  wagging progression bands between 1,198 and 1,330  $\text{cm}^{-1}$ , we were able to calculate the orientation of the all-*trans* acyl chain direction relative to the

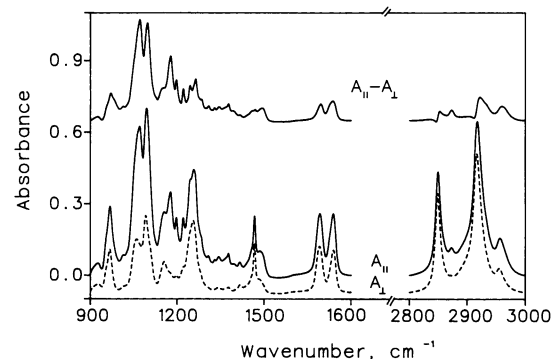


FIGURE 4 Polarized ATR-FT-IR spectra of a solid, oriented film of 2( $^{13}\text{C}$ )DMPC. Spectra were recorded with parallel ( $A_{||}$  solid trace) and perpendicular polarized light ( $A_{\perp}$  broken trace). The difference spectrum  $A_{||} - A_{\perp}$  is shown on top.

**TABLE 1** Dichroic ratio  $R$ , order parameter  $f$ , and calculated angle  $\beta$  of selected absorption bands in solid, oriented films of 2(1- $^{13}\text{C}$ ) DMPC and 2(1- $^{13}\text{C}$ ) DPPC

Assignment	2(1- $^{13}\text{C}$ ) DMPC				2(1- $^{13}\text{C}$ ) DPPC			
	Wavenumber $\text{cm}^{-1}$	$R$	$f$	$\beta$	Wavenumber $\text{cm}^{-1}$	$R$	$f$	$\beta$
$\nu\text{CH}_2$ sym.	2,850	1.03	0.82*	22°*	2,850	1.05	0.76*	23.5°*
$\nu\text{C}=\text{O}$ ( <i>sn</i> -1)	1,740	1.4	-0.21	64°	1,739	1.45	-0.19	63°
$\nu^{13}\text{C}=\text{O}$ ( <i>sn</i> -2)	1,693	1.33	-0.24	65.5°	1,694	1.35	-0.23	65°
$\text{CH}_2$ scissoring	1,467	1.04	0.8*	23.0°*	1,467	1.05	0.76*	23.5°*
$\text{CH}_2$ wagging band progression	1,203, 1,229, 1,253 1,278, 1,304, 1,328	$\geq 9$	$\geq 0.67$	$\leq 28^\circ$	1,198, 1,219, 1,242, 1,265, 1,287, 1,310, 1,330	$\geq 8$	$\geq 0.63$	$\leq 29^\circ$
$\nu\text{PO}_2^-$ asym.	1,255	1.1	-0.35	72°	1,255	1.2	-0.3	69°
$\nu\text{C}-\text{O}$ ( <i>sn</i> -1)	1,179	$\geq 10$	$\geq 0.7$	$\leq 26^\circ$	1,178	$\geq 9$	$\geq 0.67$	$\leq 28^\circ$
$\nu^{13}\text{C}-\text{O}$ ( <i>sn</i> -2)	1,153	1.45	-0.19	63°	1,153	1.5	-0.17	62°
$\nu\text{PO}_2^-$ sym.	1,092	2.05	0.02	54°	1,193	2.02	0	54.5°
$\nu\text{C}-\text{O}-\text{PO}_2^-$	1,060-1,071	2.9	0.21	46.5°	1,060-1,072	2.7	0.17	48°
$\nu\text{N}^+(\text{CH}_3)_3$ asym.	970	1.58	-0.14	60.5°	970	1.55	-0.15	61°

\*The order parameter  $f$  and the angle  $\beta$  are values for the all-*trans* hydrocarbon chains (see also Appendix).

membrane normal. The average deviation of the hydrocarbon chains from the normal to the bilayer plane is  $25 \pm 3^\circ$  for both DMPC and DPPC. This value is in good agreement with earlier infrared investigations of unlabeled DMPC (16) and DPPC (13). From an inspection of the dichroic ratios of the *sn*-1 and *sn*-2 C=O bands at 1,740 and 1,694  $\text{cm}^{-1}$  in dry 2(1- $^{13}\text{C}$ )DPPC and 2(1- $^{13}\text{C}$ )DMPC (see Table 1 and Figs. 4 and 5), it is evident that both C=O groups are equally oriented with respect to the bilayer normal. The calculated angle  $\beta$  is  $64 \pm 1^\circ$

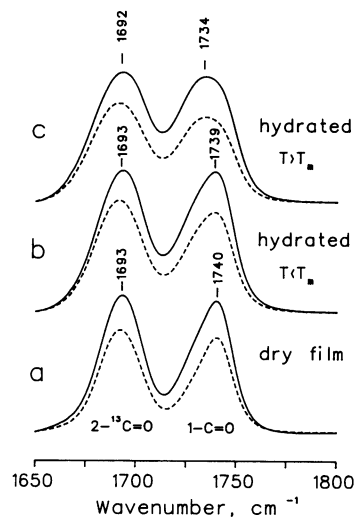


**FIGURE 5** Polarized ATR-FT-IR spectra, in the region of the C=O stretching bands, of oriented films of 2(1- $^{13}\text{C}$ )DMPC in the solid state (a), and when hydrated (with  $\text{D}_2\text{O}$ ) below (b) and above (c) the phase transition temperature  $T_m$ . Solid and broken traces represent spectra recorded with parallel and perpendicular polarized light, respectively.

for both the *sn*-1  $^{12}\text{C}=\text{O}$  and the *sn*-2  $^{13}\text{C}=\text{O}$  group in the solid phosphatidylcholine films, indicating that these groups are aligned parallel to the bilayer plane.

The question arises as to how the presence of water affects the orientation of the ester C=O bonds in fully hydrated lipid multilayers. Fig. 5 shows a comparison of the infrared spectrum in the carbonyl stretching region, recorded with parallel ( $A_{\parallel}$ ) and perpendicular ( $A_{\perp}$ ) polarized light, of 2(1- $^{13}\text{C}$ )DMPC as a solid dry film, with the spectra of hydrated films below and above the gel to liquid-crystalline phase transition temperature ( $T_m = 24^\circ\text{C}$ ). The relative intensities of the *sn*-1  $^{12}\text{C}=\text{O}$  and *sn*-2  $^{13}\text{C}=\text{O}$  bands recorded with  $A_{\parallel}$  and  $A_{\perp}$  polarizations are very similar in all three physical states of the lipid. From these spectra it is obvious that the orientation of the two ester C=O groups does not change drastically. A noteworthy difference, however, is an increase in intensity on the low frequency side of the *sn*-1 C=O band when the sample is in the hydrated state, which even results in a shift of the overall peak maximum from 1,739  $\text{cm}^{-1}$  to 1,734  $\text{cm}^{-1}$  above the gel to liquid-crystalline phase transition temperature. We believe that the reason for the change in the overall shape of the carbonyl absorption bands is hydrogen bonding of water molecules to the C=O groups, which results in the appearance of a low frequency component band at 1,725  $\text{cm}^{-1}$ , besides the band at 1,740  $\text{cm}^{-1}$  due to the free carbonyl group (23). The free and hydrogen-bonded component bands of the *sn*-1 C=O group can be resolved by band narrowing techniques such as Fourier self deconvolution or derivation (24 and references therein). The apparent frequency shift at  $T_m$  is, in our view, a result of the increased intensity of the low

frequency component due to increased hydrogen bonding (23, 25). Interestingly, the orientation of the C=O groups relative to the z-axis is not affected by hydrogen bonding to water. Band simulations of the *sn*-1 C=O bandshape with two underlying bands at 1,725 and 1,740  $\text{cm}^{-1}$  indicate the same relative intensity ratio  $A_{\parallel}/A_{\perp}$  for both bands.

At this point we have to remark that the appearance in DPPC of a carbonyl band at 1,725  $\text{cm}^{-1}$  was also interpreted in a different way. Raman spectroscopic investigations of Bicknell-Brown and Brown (26) of dry and unlabeled DPPC revealed two C=O bands in the crystalline state. The band at 1,740  $\text{cm}^{-1}$  was assigned to the *sn*-2 and the band at 1,725  $\text{cm}^{-1}$  to the *sn*-1 carbonyl moiety. Their interpretation was conformational non-equivalence of the two acyl chains of DPPC in the crystalline state. Only one band was found in the molten state, which was interpreted as conformational equivalence of the two chains. A subsequent infrared spectroscopic study of specifically  $^{13}\text{C}=\text{O}$  labeled DPPC in the dry and in the hydrated state, performed by Green et al. (27), already showed that this assignment was incorrect. However, as distinct from both groups, we interpret the C=O bands observed in the dry films of 2(1- $^{13}\text{C}$ )DPPC at 1,736 and 1,724  $\text{cm}^{-1}$  for the *sn*-1 chain and at 1,695 and 1,681  $\text{cm}^{-1}$  for the *sn*-2 chain (reference 27), as well as the bands at 1,740 and 1,725  $\text{cm}^{-1}$ , observed in the crystalline nonlabeled DPPC (reference 26), not as conformational inequivalence within a given molecule, but as a result of interchain interactions between neighboring molecules in an orthorhombic lattice, which leads to a crystal field splitting of the C=O frequencies. The crystal field splitting should not occur, or be strongly attenuated, when the molecules are arranged in a quasihexagonal lattice and the acyl chains can rotate around their long axis, or if the interchain interactions are diminished for some other reason.

Next we performed a detailed investigation of the temperature dependence of the dichroic ratio of the *sn*-1 C=O and *sn*-2  $^{13}\text{C}=\text{O}$  stretching bands in fully hydrated 2(1- $^{13}\text{C}$ )DMPC and 2(1- $^{13}\text{C}$ )DPPC films with the aim to search for potential differences between DMPC and DPPC, and to study temperature-induced changes. The results are illustrated in Fig. 6. Fig. 6A shows the temperature dependence of the symmetric  $\text{CH}_2$  stretching vibration in fully hydrated 2(1- $^{13}\text{C}$ )DMPC and 2(1- $^{13}\text{C}$ )DPPC films. This band is of high diagnostic value as it reveals the phase state of the multilamellar lipid layers deposited on the germanium crystal. The shift in frequency of the symmetric  $\text{CH}_2$  stretching vibration by more than two wavenumbers (from 2,850 to 2,852/2,853  $\text{cm}^{-1}$ ), at 24°C in (2[1- $^{13}\text{C}$ ]DMPC) and at 41°C in (2[1- $^{13}\text{C}$ ]DPPC), is indicative of a gel to liquid-crystalline phase transition in fully hydrated lipids (28), and reflects

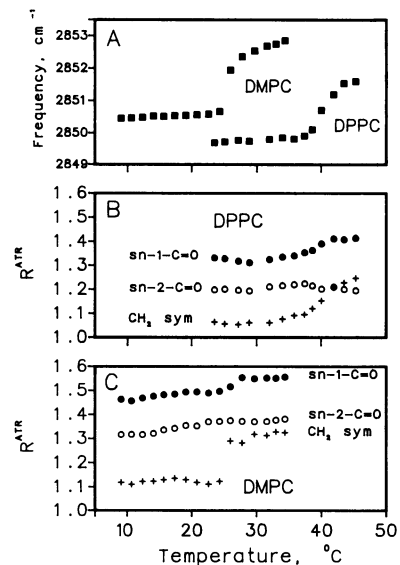


FIGURE 6 Representation of the temperature dependence of various IR spectroscopic parameters in macroscopically oriented, fully hydrated multilayers of 2(1- $^{13}\text{C}$ )DMPC and 2(1- $^{13}\text{C}$ )DPPC. (A) Frequency vs. temperature plots of the symmetric  $\text{CH}_2$  stretching bands in DMPC and DPPC. (B and C) Dichroic ratio vs. temperature plots of the two ester C=O double bond vibrations (circles) and of the symmetric  $\text{CH}_2$  stretching vibrations (+) in 2(1- $^{13}\text{C}$ )DPPC (B) and in 2(1- $^{13}\text{C}$ )DMPC (C). Full circles always represent *sn*-1  $^{13}\text{C}=\text{O}$  groups and open circles *sn*-2  $^{13}\text{C}=\text{O}$  groups.

the introduction of disorder in the hydrocarbon chains by formation of gauche conformers. Fig. 6, B and C show the dichroic ratios of various infrared bands of (2[1- $^{13}\text{C}$ ]DMPC) and (2[1- $^{13}\text{C}$ ]DPPC) as a function of temperature. From these  $R$  values one can calculate the order parameter  $f$  and the orientation of individual functional groups. Thus, a dichroic ratio  $R$  of 1.1 is obtained for the symmetric  $\text{CH}_2$  stretching vibration of both lipids. From this  $R$  value we calculate an order parameter of  $f = 0.7$ , and an average chain tilt of  $26^\circ$  relative to the bilayer normal (for details see Appendix). At  $T_m$  the  $R$  value increases from 1.1 to 1.3, which is equivalent to a decrease in the order parameter to  $f = 0.5$ . This, however, is not owing to a further increase of the chain tilt, but due to the introduction of gauche conformers in the all-*trans* zig-zag methylene chains which brings the average  $\text{CH}_2$  transition moment closer to the direction of the z-axis (or the bilayer normal). In 2(1- $^{13}\text{C}$ )DPPC, a slight increase in  $R$  is detected in the  $P_B$  phase above the pretransition temperature of 33°C (see Fig. 6B). The same can be seen above the pretransition temperature of 2(1- $^{13}\text{C}$ )DMPC in the  $P_B$ -phase between 14 and 20°C (see Fig. 6C). Then, between 20 and 24°C the  $R$  ratio decreases slightly. It is difficult to calculate an average chain tilt in the ripple ( $P_B$ ) phase because a small

increase in disorder of the acyl chains (produced, for example, by a small amount of gauche conformers with a concomitant small reduction of the chain tilt), would not alter the observed  $R$  values considerably. Therefore, the chain tilt can be calculated most precisely for the hydrated gel state of the phosphatidylcholines below their pretransition temperature, in the  $L_B$  phase in which we can assume nearly perfect all-*trans* conformation of the acyl chains.

The  $R$  values obtained for the *sn*-2 carbonyl band of  $2(1-^{13}\text{C})\text{DMPC}$  and  $2(1-^{13}\text{C})\text{DPPC}$  do not change at the gel to liquid-crystalline phase transition temperature, indicating that the orientation of the *sn*-2  $\text{C}=\text{O}$  group is the same below and above  $T_m$ . On the other hand, the temperature profile of the dichroic ratio of the *sn*-1  $\text{C}=\text{O}$  group in both DMPC and DPPC (filled circles, Fig. 6, *B* and *C*) follows the behavior of the symmetric  $\text{CH}_2$  stretching mode, but the increase in the dichroic ratio at  $T_m$  is smaller ( $\Delta R \leq 0.05$ ). This change in  $R$  only results in a minor change of the average orientation of the *sn*-1 carbonyl group by 1 or  $2^\circ$ . We believe that this minor change reflects a somewhat less ordered alignment of the *sn*-1  $\text{C}=\text{O}$  group relative to the  $z$ -axis, caused by the larger number of gauche conformers and the increased motional freedom of the methylene groups of the *sn*-1 chain above  $T_m$ . In  $2(1-^{13}\text{C})\text{DPPC}$  the order parameter of the *sn*-1  $\text{C}=\text{O}$  group ranges from  $f = -0.24$  ( $\beta = 66^\circ$ ) in the gel phase, to  $-0.21$  ( $\beta = 64^\circ$ ) in the liquid-crystalline phase, whereas for the *sn*-2  $\text{C}=\text{O}$  group  $f$  is always  $-0.29$  ( $\beta = 68^\circ$ ). In  $2(1-^{13}\text{C})\text{DMPC}$  the  $f$  value of the *sn*-1  $\text{C}=\text{O}$  bond is  $-0.18$  ( $\beta = 62.5^\circ$ ) in the gel phase, and  $-0.15$  ( $\beta = 61^\circ$ ) in the  $L_a$  phase, whereas the roughly constant  $R$  value of 1.35 for the *sn*-2  $\text{C}=\text{O}$

bond results in an order parameter  $f = -0.24$  ( $\beta = 65^\circ$ ) over the entire temperature range investigated. A closer inspection of Fig. 6 *C* reveals a small increase in the dichroic ratio of the *sn*-2  $\text{C}=\text{O}$  group of  $2(1-^{13}\text{C})\text{DMPC}$  from 1.33 to 1.37 between 14 and  $23^\circ\text{C}$  ( $P_B$  phase) which accounts for a change of  $< 1^\circ$  in the angle  $\beta$ . Certainly the orientation of the two carbonyl groups relative to the  $z$ -axis is far from random (or the magic angle orientation of  $\beta = 54.7^\circ$ ), otherwise the dichroic ratio should exhibit a value  $\sim 2$ , resulting in an order parameter of  $f = 0$ .

The calculated  $\beta$  values for the two ester  $\text{C}=\text{O}$  bonds in  $2(1-^{13}\text{C})\text{DMPC}$  and  $2(1-^{13}\text{C})\text{DPPC}$  are given in Table 2. In the two investigated hydrated phosphatidylcholines, the *sn*-1  $\text{C}=\text{O}$  group is on average oriented at  $64 \pm 2^\circ$  relative to the bilayer plane in the gel phase, and at  $62 \pm 2^\circ$  in the liquid-crystalline phase. For the *sn*-2  $\text{C}=\text{O}$  group, this angle  $\beta$  is always slightly higher and independent of the phase state of the bilayer ( $\beta = 66 \pm 2^\circ$ ).

Further information about the structural arrangement of segments of the polar headgroup and the hydrocarbon chains can be extracted from infrared spectra in the region  $1,000\text{--}1,300\text{ cm}^{-1}$ . Fig. 7 shows the ATR-IR spectra in this region of dry and hydrated  $2(1-^{13}\text{C})\text{DMPC}$ , recorded with parallel and perpendicular polarized light. In the dry lipid the antisymmetric phosphate ( $\text{PO}_2^-$ ) vibration is found at  $1,255\text{ cm}^{-1}$ , in the hydrated state it shifts to  $1,229\text{ cm}^{-1}$  as a consequence of hydrogen bonding to water molecules (14). In the  $A_{\parallel}$  polarization of dry and hydrated gel phase spectra (solid traces, Figs. 7, *a* and *b*) this band overlaps with three of the six  $\text{CH}_2$  wagging bands (at  $1,230$ ,  $1,256$ , and  $1,280\text{ cm}^{-1}$ ) which originate from the all-*trans* methylene groups of

TABLE 2 Dichroic ratio  $R$ , order parameter  $f$ , and calculated angle  $\beta$  of selected absorption bands in hydrated phosphatidylcholine films

Assignment	$T < T_m$				$T > T_m$			
	Wavenumber	$R$	$f$	$\beta$	Wavenumber	$R$	$f$	$\beta$
	$\text{cm}^{-1}$				$\text{cm}^{-1}$			
$\nu\text{OH}$ ( $\text{H}_2\text{O}$ )	3,400	2.0	0	Random	3,400	2.0	0	Random
$\nu\text{CH}_2$ sym.	2,850	1.1	0.7*	$26^\circ$ *	2,852.5	1.3	0.54*	—
$\nu\text{OD}$ ( $\text{D}_2\text{O}$ )	2,490	2.0	0	Random	2,490	2.0	0	Random
$\nu\text{C}=\text{O}$ ( <i>sn</i> -1)	1,739	$1.4 \pm 0.06$	$-0.2 \pm 0.03$	$64 \pm 2^\circ$	1,734	$1.47 \pm 0.08$	$-0.18 \pm 0.04$	$62 \pm 2^\circ$
$\nu^{13}\text{C}=\text{O}$ ( <i>sn</i> -2)	1,693	$1.28 \pm 0.08$	$-0.26 \pm 0.03$	$66 \pm 2^\circ$	1,692	$1.28 \pm 0.08$	$-0.26 \pm 0.03$	$66 \pm 2^\circ$
$\nu\text{PO}_2^-$ asym.	1,230	1.1	-0.35	$72^\circ$	1,229	1.3	-0.27	$66^\circ$
$\text{CH}_2$ wagging	1,203/1,198†	$\geq 8$	$\geq 0.63$	$\leq 29^\circ$	<i>b</i>	<i>b</i>	<i>b</i>	<i>b</i>
$\nu\text{CO}-\text{O}$ ( <i>sn</i> -1)	1,178	7	0.59	$31^\circ$	1,175	4	0.37	$40^\circ$
$\nu^{13}\text{CO}-\text{O}$ ( <i>sn</i> -2)	1,153	1.55	-0.15	$61^\circ$	1,148	1.55	-0.15	$61^\circ$
$\nu\text{PO}_2^-$ sym.	1,090	1.9	-0.03	$56^\circ$	1,089	1.9	-0.03	$56^\circ$
$\nu\text{N}^+(\text{CH}_3)_3$ asym.	970	1.8	-0.06	<i>a</i>	970	1.75	-0.08	<i>a</i>

\*The order parameter  $f$  and the angle  $\beta$  are values for the all-*trans* hydrocarbon chains (see also Appendix).

†Head bands of the wagging band progression in DMPC/DPPC.

*a* Probably nearly random orientation.

*b* Not observable.

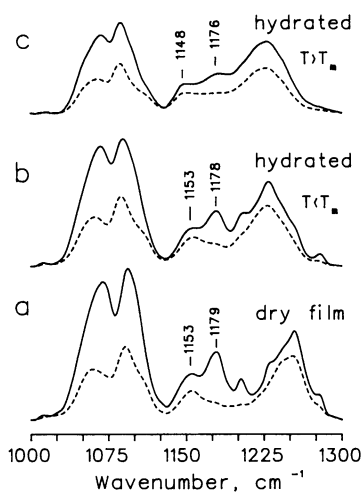


FIGURE 7 Polarized ATR-FT-IR spectra, in the region 1,000–1,300  $\text{cm}^{-1}$  of macroscopically oriented 2(1- $^{13}\text{C}$ )DMPC films in the solid state (a), and when hydrated (with  $\text{H}_2\text{O}$ ) below (b) and above (c) the phase transition temperature  $T_m$ . Solid and broken traces represent spectra recorded with parallel and perpendicularly polarized light, respectively. The frequencies of the two ester CO—O single bond vibrations are marked.

the myristoyl chains. In the  $A_{\perp}$  polarized spectra (broken traces, Figs. 7, a and b) these  $\text{CH}_2$  wagging bands are hardly visible. The high dichroic ratio of these bands (see Tables 1 and 2) translates into a tilt angle of the hydrocarbon chains of  $<30^\circ$  relative to the bilayer normal, which agrees well with the tilt angle derived from the  $R$  values of the symmetric  $\text{CH}_2$  stretching vibration. In the liquid-crystalline phase, the  $\text{CH}_2$  wagging band progression is absent owing to the high number of gauche conformers. Similar results were found for 2(1- $^{13}\text{C}$ )DPPC, with the exception that the  $\text{CH}_2$  wagging progression in the range 1,198–1,330  $\text{cm}^{-1}$  consists of seven bands (see Table 2).

The dichroic ratio of the antisymmetric  $\text{PO}_2^-$  stretching vibration is  $\sim 1.1$  in the dry film and in the gel phase of both lipids, resulting in an average angle of  $\beta = 72^\circ$ . In the liquid-crystalline phase  $R$  increases to 1.3 ( $\beta = 66^\circ$ ). Thus, the transition moment of this vibration (directed along the connecting line of the two nonesterified phosphate oxygens) lies preferentially in the bilayer plane. The transition moment of the symmetric  $\text{PO}_2^-$  stretching (band at  $\sim 1,090 \text{ cm}^{-1}$ ) is oriented parallel to the bisector of the  $\text{O}=\text{P}-\text{O}$  angle. This band shows a dichroic ratio of  $R = 2.0$  in dry films and 1.9 in the hydrated state of both lipids. From the calculated order parameter  $f \sim 0$  we must conclude that the average transition moment of the symmetric  $\text{PO}_2^-$  vibration lies either at  $\sim 55^\circ$  relative to the bilayer normal, or that this transition moment is randomly oriented. As the transi-

tion moments of the symmetric and antisymmetric phosphate vibration are both located in the  $\text{PO}_2^-$  plane (though perpendicular to each other), and because they have different dichroic ratios, a random orientation of this molecular fragment can be excluded, even in the liquid-crystalline phase. For the same reason, a radial distribution or rotation of the  $\text{PO}_2^-$  group around the  $\text{C}-\text{O}-(\text{PO}_2^-)-\text{O}-\text{C}$  phosphodiester axis also seems unlikely.

The most important feature in Fig. 7 is the dichroic behavior of the ester CO—O single bonds. The C—O stretching band at 1,179  $\text{cm}^{-1}$ , which originates from the *sn*-1  $\text{CH}_2\text{CO}-\text{O}$  fragment, shows strong  $z$ -polarization in the dry film and the hydrated gel state, resulting in an average tilt angle of this transition moment of  $\sim 30^\circ$  relative to the bilayer normal. This is the same tilt angle as that of the acyl chains (see Tables 1 and 2). At  $T_m$  the dichroic ratio of the *sn*-1 CO—O stretching band changes from  $\sim 7$  to  $\sim 4$ , meaning that the tilt angle  $\beta$  changes from  $\sim 31^\circ$  to  $\sim 40^\circ$  relative to the bilayer normal. Concomitantly, the frequency maximum shifts from 1,179 to 1,175  $\text{cm}^{-1}$ . This decrease in the order parameter from  $f = +0.6$  to  $f = +0.37$  could be a consequence of the introduction of gauche conformers in the neighbouring methylene groups, and/or a higher mobility of the lipid molecules, caused by torsional motions and director fluctuations of the chain axes. Infrared experiments on crystalline and molten tripalmitin (29) showed that when the  $\text{C}-\text{O}-\text{C}_1\text{O}-\text{C}_2-\text{C}_3$  segments of the ester chains adopt a planar all-*trans* conformation the CO—O single bond vibration appears at 1,180  $\text{cm}^{-1}$ , but if the dihedral angle  $\text{O}-\text{C}_1\text{O}-\text{C}_2-\text{C}_3$  deviates from  $180^\circ$ , as in the disordered state of molten tripalmitin, then this band shifts to  $\sim 1,170 \text{ cm}^{-1}$ . We have observed the same behavior with the model ester compound methyl palmitate (see above). Hence, the presence of a band at 1,178  $\text{cm}^{-1}$  in dry and hydrated 2(1- $^{13}\text{C}$ )DMPC and 2(1- $^{13}\text{C}$ )DPPC points to an all-*trans* conformation of the *sn*-1 chain up to the glycerol carbon atom, and the frequency shift to 1,175  $\text{cm}^{-1}$  in the liquid-crystalline phase may be interpreted as a slight deviation from the dihedral angle of  $180^\circ$  in this segment, induced by torsional motions or by a small population of gauche conformers near the *sn*-1 CO—O single bond.

In contrast to the high  $z$ -polarization of the *sn*-1 CO—O single bond vibration, the ester *sn*-2  $^{13}\text{CO}-\text{O}$  single bond vibration of 2(1- $^{13}\text{C}$ )DMPC and 2(1- $^{13}\text{C}$ )DPPC (which occurs at 1,153  $\text{cm}^{-1}$ ) exhibits an  $R$  value of 1.5 both in the dry film and the hydrated gel state. From the  $R$  value one obtains an order parameter  $f = -0.17$ , and thus a tilt angle of  $\beta = 62^\circ$  relative to the bilayer normal. The dichroic ratio of the *sn*-2 CO—O single bond vibration does not change significantly at  $T_m$



( $R = 1.55$ ). In the liquid crystalline phase, however, the calculated order parameter of  $f = -0.15$  is quite different from that obtained for the *sn*-1 CO—O single bond vibration ( $f = +0.37$ ). In the gel phase these differences are even larger (*sn*-1 CO—O,  $f = +0.59$  and *sn*-2  $^{13}\text{CO—O}$ ,  $f = -0.15$ ). From the experimentally determined orientation of the transition moment of this vibration, and the known geometry of the  $\text{CH}_2\text{CO—O}$  molecular frame, we must conclude that both in the gel phase and in the liquid-crystalline phase, the fragment connected to the glycerol  $\text{C}_1$  atom is oriented toward the bilayer normal, whereas the  $\text{CH}_2\text{CO—O}$  fragment connected to the *sn*-2 glycerol carbon atom is oriented toward the bilayer plane. Consequently, the glycerol moiety has to adopt an orientation nearly parallel to the  $z$ -axis (or the membrane normal), with a tilt angle of  $30 \pm 10^\circ$ .

Because the *sn*-2 chain first extends parallel to the bilayer plane, a conformation with a bend at the  $\text{C}_2\text{—C}_3$  bond (as was shown in the crystal structure of DMPC), must also exist in the hydrated state to accommodate parallel chain alignment in the bilayer. Infrared spectroscopic evidence for such a bend comes from the frequency of the *sn*-2  $^{13}\text{CO—O}$  single bond vibration. As was mentioned earlier, this vibration is coupled with the  $\alpha\text{CH}_2$  bending mode, therefore any conformational change near the  $\alpha\text{CH}_2$  group of this acyl chain should also affect the frequency of the respective CO—O single bond vibration. We have shown that when the fragment  $\text{C}_3\text{—C}_2\text{—}^{13}\text{CO—O}$  of the model ester compound methyl( $1\text{-}^{13}\text{C}$ )palmitate is in a planar, all-*trans* zig-zag conformation (dihedral angle  $180^\circ$ ), the  $^{13}\text{CO—O}$  single bond vibration occurs at  $1,158\text{ cm}^{-1}$ . Rotation around the  $\text{C}_2\text{—}^{13}\text{CO}$  bond leads to nonplanarity and to a shift in the frequency of this band to  $1,152\text{ cm}^{-1}$  (see Figs. 1 and 2). In the dry film and the hydrated gel phases of  $2(1\text{-}^{13}\text{C})\text{DMPC}$  and  $2(1\text{-}^{13}\text{C})\text{DPPC}$  the *sn*-2  $^{13}\text{CO—O}$  single bond vibration indeed appears at  $1,153\text{ cm}^{-1}$ , which may be explained by *gauche* conformers around the  $\text{C}_2\text{—}^{13}\text{CO}$ -bond ( $\text{C}_3\text{—C}_2\text{—}^{13}\text{CO—O}$  dihedral angle  $\sim 120^\circ$  or  $\sim 60^\circ$ ). Surprisingly, we observe a further decrease in frequency of this band at the phase transition temperatures of  $2(1\text{-}^{13}\text{C})\text{DMPC}$  and  $2(1\text{-}^{13}\text{C})\text{DPPC}$ , from  $1,153$  to  $1,148\text{ cm}^{-1}$ . At present, we do not have a straightforward explanation for this phenomenon. However, because the orientation of the transition moment of the *sn*-2 CO—O single bond vibration does not change simultaneously, we presume that either rapid conformational changes around the  $\text{C}_2\text{—}^{13}\text{CO}$  bond of the *sn*-2 chain (movement of the  $\text{C}_2\text{—C}_3$  bond relative to a fixed CO—O frame), or hydrogen-bonding effects are responsible for this shift in frequency.

## DISCUSSION

This is the first direct measurement of the orientation of individual *sn*-1 and *sn*-2 C=O double bonds and *sn*-1 and *sn*-2 CO—O single bonds in hydrated diacyl phosphatidylcholines in the gel phase and in the liquid-crystalline phase. The results presented herein show unambiguously that in phosphatidylcholine multilayers both ester carbonyl double bonds are aligned in the membrane plane with a tilt angle  $\beta$  relative to the bilayer normal greater than  $60^\circ$ . No significant differences were detected between the orientation of the *sn*-1 and *sn*-2 C=O bonds in dry films of DMPC and DPPC and in hydrated films at temperatures below and above the respective phase transitions. Differences in the orientation of the *sn*-1 and *sn*-2 C=O ester bonds exist, however, in the crystalline  $\text{L}_c$  phase of diacyl phospholipids (Hübner, W., N. H. Lewis, R. N. McElhaney, and H. H. Mantsch, manuscript in preparation).

On the other hand, the transition moments of the two ester CO—O single bond vibrations are oriented very differently within the bilayer of the two investigated phosphatidylcholines DMPC and DPPC. In the solid state, and in the aqueous gel phase, the  $\text{CH}_2\text{CO—O}$  segment of the *sn*-1 chain is oriented along the all-*trans* methylene chain, whereas the same segment of the *sn*-2 chain is oriented in the bilayer plane.

As a consequence of the different orientations of the *sn*-1 and *sn*-2 CO—O single bonds, the glycerol moiety has to be oriented nearly perpendicular to the membrane plane and a  $90^\circ$  bend must exist near the  $\text{C}_2$  carbon of the *sn*-2 chain in order that the chains become parallel. Infrared spectroscopic evidence for such a bend conformation comes from the frequency of the *sn*-2  $\text{CH}_2\text{CO—O}$  single bond vibration (see Results). According to our findings, the orientational differences between the initial segments of the *sn*-1 and *sn*-2 chain are maintained in the liquid-crystalline phase. In view of this, we want to comment on a model of phospholipid bilayer structure in the liquid-crystalline state proposed by Hauser (12), in which the conformations of four different phospholipid x-ray structures are assumed to be minimum energy potentials, interconverting rapidly into each other by a change of torsional angles in and near the glycerol backbone. From our polarized ATR-IR spectra we can conclude that two structures, i.e., the conformers with a straight *sn*-2 chain and a  $90^\circ$  bend in the *sn*-1 chain have only a very low probability (if any at all) to occur in the liquid-crystalline phase of these diacyl phosphatidylcholines. However, rapid interconversion between the remaining two proposed conformations (see reference 12) derived from the x-ray structure

of DMPC and that of dilauroyl-*N,N*-dimethylethanolamine, is compatible with our experimental findings, as in both structures the bend conformation in the *sn*-2 chain and the orientation of the carbonyl groups relative to the bilayer normal, is preserved. The shift in frequency of the *sn*-2 CO—O single bond vibration at the gel to liquid-crystalline phase transition, without a concomitant change in the orientation of the respective transition moment, may in fact be interpreted as reflecting rapid changes in torsion angles around the C<sub>2</sub>—C<sub>3</sub> and C<sub>3</sub>—C<sub>4</sub> bonds of the *sn*-2 chain, which are required for the interconversion between the two proposed conformations. In view of this, the interpretation of the results of <sup>13</sup>C—NMR investigations of phosphatidylcholines in the liquid-crystalline phase (9, 11), which indicated a tensor orientation of the *sn*-2 carbonyl group relative to the rotation axis of the lipid chains (bilayer normal) close to the magic angle, have to be reconsidered. It would be worthwhile to use theoretical calculations to establish whether rapid interconversion of dihedral angles by rotation around the *sn*-2 O—OC<sub>1</sub>—C<sub>2</sub>—C<sub>3</sub>—C<sub>4</sub> bond with a relatively fixed carbonyl group, in addition to fast rotational diffusion around the bilayer normal, could account for an averaging of the tensor of the chemical shielding anisotropy, such as to produce an isotropic line in the <sup>13</sup>C—NMR spectrum. This could provide an alternative interpretation for the <sup>13</sup>C—NMR data (30, 31).

## APPENDIX

### Infrared dichroism in uniaxially oriented thick films

The dichroic ratio *R* of a given infrared absorption band is defined as the ratio of the integrated intensity of the infrared radiation polarized parallel to the plane of incidence (*A*<sub>||</sub>) to that polarized perpendicular to the plane of incidence (*A*<sub>⊥</sub>). In a Cartesian coordinate system (*x*, *y*, *z*) the incoming and the reflected IR beam determine the plane of incidence (*xz*-plane), where the *x*-axis is defined as the propagation direction of the infrared beam along the ATR crystal; the *z*-axis is then perpendicular to the surface of the ATR crystal determined by the *xy*-plane.

The angle between the incoming beam and the *z*-axis is defined as the angle of incidence  $\vartheta$ . With this definition one can write

$$R = \frac{A_{||}}{A_{\perp}} = \frac{E_x^2 \cdot k_x \cdot E_z^2 \cdot k_z}{E_y^2 \cdot k_y}, \quad (\text{A1})$$

where *E<sub>x</sub>* is the electric field amplitude in the *x*-direction and *k<sub>x</sub>* is the integrated absorption coefficient in the *x*-direction, with similar expressions for *y* and *z*.

For an uniaxial model with fiber-type orientation, Fraser (32) established an equation that relates the integrated absorption coefficients *k<sub>x</sub>*, *k<sub>y</sub>*, and *k<sub>z</sub>* with an order parameter *f*

$$k_z = K \cdot M^2 [f \cdot \cos^2 \gamma + (\frac{1}{3})(1 - f)]$$

$$k_x = k_y = K \cdot M^2 [(\frac{1}{2})f \cdot \sin^2 \gamma + (\frac{1}{3})(1 - f)], \quad (\text{A2})$$

where *K* is a constant, *M* is the transition moment per unit electric field amplitude associated with a particular infrared band, and  $\gamma$  is the angle which the transition moment makes with the fiber axis *c*. The assumption is that all directions about the *c*-axis are equally probable.

With the assumption that the lipid molecules are uniaxially oriented in the *xy*-plane of the crystal, and therefore *k<sub>x</sub>* = *k<sub>y</sub>*, Eqs. A1 and A2 may be combined to give:

$$R = \frac{E_x^2}{E_y^2} + \frac{E_z^2 [f \cdot \cos^2 \gamma + (\frac{1}{3})(1 - f)]}{E_y^2 [(\frac{1}{2})f \cdot \sin^2 \gamma + (\frac{1}{3})(1 - f)]}. \quad (\text{A3})$$

To calculate the order parameter *f* from Eq. A3 one has to determine the electric field amplitudes *E<sub>x</sub>*, *E<sub>y</sub>*, and *E<sub>z</sub>*. We have used the equations for thick films, that is thick compared with the penetration depth of the evanescent wave (33):

$$\begin{aligned} E_y &= \frac{2 \cdot \cos \vartheta}{(1 - n_{21}^2)^{1/2}} \\ E_x &= 2 \cdot \frac{(\sin^2 \vartheta - n_{21}^2)^{1/2} \cdot \cos \vartheta}{(1 - n_{21}^2)^{1/2} [(1 + n_{21}^2) \sin^2 \vartheta - n_{21}^2]^{1/2}} \\ E_z &= 2 \cdot \frac{\sin \vartheta \cdot \cos \vartheta}{(1 - n_{21}^2)^{1/2} [(1 + n_{21}^2) \sin^2 \vartheta - n_{21}^2]^{1/2}}, \end{aligned} \quad (\text{A4})$$

where *n*<sub>21</sub> = *n*<sub>2</sub>/*n*<sub>1</sub> is the ratio of the refractive index of the rare medium to that of the dense medium. Under our experimental conditions (angle of incidence  $\vartheta = 45^\circ$ , refractive index for the lipid film *n*<sub>2</sub> = 1.44 and for germanium *n*<sub>1</sub> = 4), the electric field amplitudes are *E<sub>x</sub>* = 1.398, *E<sub>y</sub>* = 1.516, and *E<sub>z</sub>* = 1.625.

From the order parameter *f*, and an uniaxial orientation of the fiber axis *c* with respect to the normal of the ATR crystal plane, we are able to calculate the mean angle  $\beta$  between our macroscopic *z*-axis (the bilayer normal) and the fiber axis *c* as

$$f(\beta) = \frac{1}{2} \cdot (3 \cos^2 \beta - 1). \quad (\text{A5})$$

In our experiments, the transition moments of the vibrations of the polar head group (i.e., the C=O double bond vibration, the PO<sub>2</sub><sup>-</sup> vibration, and the CO—O single bond vibration) and the transition moment of the CH<sub>2</sub> wagging band progression (along the direction of the all-*trans* acyl chains), are oriented along the fiber axis *c*. With  $\gamma = 0^\circ$ , *E<sub>x</sub><sup>2</sup>/E<sub>y</sub><sup>2</sup>* = 0.85 and *E<sub>z</sub><sup>2</sup>/E<sub>y</sub><sup>2</sup>* = 1.15 in Eq. A3, the order parameter *f* ( $\beta$ ) can be obtained from the experimental *R* values according to

$$f = \frac{R - 2}{R + 1.45}. \quad (\text{A6})$$

When deriving the order parameter of the lipid chain axis from the dichroic ratios *R* of the CH<sub>2</sub> stretching or CH<sub>2</sub> bending vibrations one has to use  $\gamma = 90^\circ$  in Eq. A3, meaning that the transition moments are perpendicular to the chain axis. Thus,

$$f = -2 \frac{R - 2}{R + 1.45}. \quad (\text{A7})$$

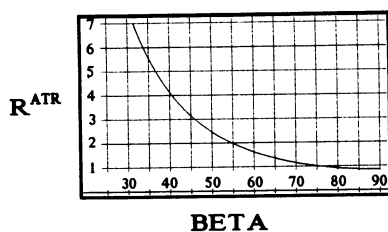


FIGURE A1 Relation between the dichroic ratio  $R$  and the angle  $\beta$  (in degrees), as derived from Eq. A8.

The order parameter  $f$  varies between  $-0.5$  for perfectly perpendicular, or in the plane of the crystal orientation ( $R = 0.85$ ), to  $f = +1$  for perfectly parallel, or perpendicular to the plane of the crystal orientation, also referred to as  $z$ -polarization ( $R \rightarrow \infty$ ). An order parameter of  $f = 0$  ( $R \approx 2$ ) may indicate either an orientation of  $\beta = 54.7^\circ$  relative to the  $z$ -axis, or completely random orientation.

We have used Eq. A6 or A7 to compute the various order parameters  $f(\beta)$ , and Eq. A5 to calculate the tilt angle  $\beta$ .

## Error analysis

Combining Eqs. A6 and A7 yields the relation between the dichroic ratio  $R$  and the mean angle  $\beta$  of the fiber axis

$$R(\beta) = \frac{2 + 0.725(3 \cos^2 \beta - 1)}{1 - 0.5(3 \cos^2 \beta - 1)}. \quad (\text{A8})$$

Fig. A1 shows Eq. A8 in graphical form. The errors resulting from the experimental determination of  $R$  when  $1 \leq R \leq 7$  are smaller than the linewidth of the function  $R(\beta)$  in Fig. A1 ( $\Delta R \leq 0.03$ ). Under the assumption of a planar bilayer arrangement, the determination of the angle  $\beta$  is therefore highly accurate, i.e., with errors  $\Delta\beta$  of less than one degree. Only at very large dichroic ratios (i.e.,  $R \geq 7$ ) does  $\Delta R$  increase and the estimation of  $\beta$  becomes less accurate because the integrated intensity of the absorption bands recorded with perpendicular polarization is very low, which leads to a greater uncertainty in the determination of  $R$  and  $\beta$ . In these cases the values of  $R$ ,  $f$ , and  $\beta$  in Tables 1 and 2 represent only lower or upper limits. A different type of error might be introduced by choosing the same refractive index ( $n_1 = 1.44$ ) for both the dry and the hydrated film. However, because a change of  $n_1$  by  $\pm 0.05$  has only a minor effect on the calculation of the electric field amplitudes  $E_x$ ,  $E_y$ , and  $E_z$  ( $\Delta E \leq 1\%$ ), this uncertainty in the refractive index is negligible for the calculation of the angle  $\beta$ .

Issued as National Research Council Canada publication no. 32299. Dr. Hübner was a Lynen Research Fellow of the Humboldt Foundation.

Received for publication 19 October 1990 and in final form 18 January 1991.

## REFERENCES

- Pearson, R. H. and I. Pascher. 1979. The molecular structure of lecithin dihydrate. *Nature (Lond.)* 281:499–501.
- Hitchcock, P. B., R. Mason, K. M. Thomas, and G. G. Shipley.

1974. Structural chemistry of 1,2-dilauroyl-*DL*-phosphatidylethanolamine: molecular conformation and intermolecular packing of phospholipids. *Proc. Natl. Acad. Sci. USA* 71:3036–3040.
3. Büldt, G., and J. Seelig. 1980. Conformation of phosphatidylethanolamine in the gel phase as seen by neutron diffraction. *Biochemistry* 19:6170–6175.
4. Büldt, G., H. U. Gally, J. Seelig, and G. Zaccai. 1979. Neutron diffraction studies on phosphatidylcholine model membranes I. Head group conformation. *J. Mol. Biol.* 134:673–691.
5. Zaccai, G., G. Büldt, A. Seelig, and J. Seelig. 1979. Neutron diffraction studies on phosphatidylcholine model membranes. II. Chain conformation and segmental disorder. *J. Mol. Biol.* 134:691–706.
6. Seelig, A., and J. Seelig. 1975. Bilayers of dipalmitoyl-3-*sn*-phosphatidylcholine. Conformational differences between the fatty acyl chains. *Biochim. Biophys. Acta* 406:1–5.
7. Seelig, J., and J. L. Browning. 1978. General features of phospholipid conformation in membranes. *FEBS (Fed. Eur. Biochem. Soc.) Lett.* 92:41–44.
8. Schindler, H., and J. Seelig. 1975. Deuterium order parameters in relation to thermodynamic properties of a phospholipid bilayer. A statistical mechanical interpretation. *Biochemistry* 14:2283–2287.
9. Wittebord, R. J., C. F. Schmidt, and R. G. Griffin. 1981. Solid state carbon-13 NMR of the lecithin gel to liquid-crystalline phase transition. *Biochemistry* 20:4223–4228.
10. Cornell, B. A. 1986. Chemical shielding tensors of  $^{13}\text{C}$  in solid dimethyl oxalate. *J. Chem. Phys.* 85:4199–4201.
11. Braach-Maskvytis, V. L. B., and B. A. Cornell. 1988. Chemical shift anisotropies obtained from aligned egg yolk phosphatidylcholine by solid-state  $^{13}\text{C}$  NMR. *Biophys. J.* 53:839–843.
12. Hauser, H., I. Pascher, and S. Sundell. 1988. Preferred conformation and dynamics of the glycerol backbone in phospholipids. An NMR and x-ray single-crystal analysis. *Biochemistry* 27:9166–9174.
13. Fringeli, U. P. 1977. The structure of lipids and proteins studied by attenuated total reflection infrared spectroscopy. Oriented layers of a homologous series of phosphatidylethanolamine to phosphatidylcholine. *Z. Naturforsch.* 32c:20–45.
14. Akutsu, H., M. Ikematsu, and Y. Kyogoku. 1981. Molecular structure and interaction of dipalmitoyl phosphatidylcholine in multilayers. Comparative study with phosphatidylethanolamine. *Chem. Phys. Lipids* 28:149–158.
15. Holmgren, A., L. B.-A. Johansson, and G. Lindblom. 1987. An FT-IR linear dichroism study of lipid membranes. *J. Phys. Chem.* 91:5298–5301.
16. Ter-Minassian-Sarage, L., E. Okamura, J. Umemura, and T. Takenaka. 1988. FT-IR ATR spectroscopy of hydration of dimyristoylphosphatidylcholine multibilayers. *Biochim. Biophys. Acta* 946:417–423.
17. Okamura, E., J. Umemura, and T. Takenaka. 1990. Orientation studies of hydrated dipalmitoylphosphatidylcholine multibilayers by polarized FT-IR ATR spectroscopy. *Biochim. Biophys. Acta* 1025:94–98.
18. Mason, J. T., A. V. Broccoli, and C-H. Huang. 1981. A method for the synthesis of isomerically pure saturated mixed-chain phosphatidylcholines. *Anal. Biochem.* 113:96–101.
19. Jones, R. N. 1962. The effects of chain length on the infrared spectra of fatty acids and methyl esters. *Can. J. Chem.* 40:321–333.

- 
20. Jones, R. N. 1962. The infrared absorption spectra of deuterated esters. III Methyl laurate. *Can. J. Chem.* 40:301–320.
  21. Bradbury, E. M., A. Elliott, and R. D. B. Fraser. 1960. Infrared dichroism and crystallinity in polyethylene and polyethylene suberate. *Trans. Faraday Soc.* 56:1117–1124.
  22. Fringeli, U. P., and Hs. H. Günthard. 1981. Infrared membrane spectroscopy. *Mol. Biol. Biochem. Biophys.* 31:270–332.
  23. Blume, A., W. Hübner, and G. Messner. 1988. Fourier transform infrared spectroscopy of  $^{13}\text{C}=\text{O}$  labeled phospholipids. Hydrogen bonding to carbonyl groups. *Biochemistry.* 27:8239–8249.
  24. Mantsch, H. H., D. J. Moffatt, and H. L. Casal. 1988. Fourier transform methods for spectral resolution enhancement. *J. Mol. Struct.* 173:285–298.
  25. Hübner, W., H. H. Mantsch, and H. L. Casal. 1990. Beware of frequency shifts. *Appl. Spectrosc.* 44:732–734.
  26. Bicknell-Brown, E., and K. G. Brown. 1984. Raman temperature study of conformational changes in anhydrous dipalmitoylphosphatidylcholine. *Biochim. Biophys. Acta.* 778:317–323.
  27. Green, P. M., J. T. Mason, T. J. O'Leary, and I. W. Levin. 1987. Effects of hydration, cholesterol, amphotericin B, and cyclosporin A on the lipid bilayer interface region: an infrared spectroscopic study using 2-(1- $^{13}\text{C}$ ) dipalmitoylphosphatidylcholine. *J. Phys. Chem.* 91:5099–5103.
  28. Casal, H. L., and H. H. Mantsch. 1984. Polymorphic phase behaviour of phospholipid membranes studied by infrared spectroscopy. *Biochim. Biophys. Acta.* 779:381–401.
  29. Fringeli, U. P., H. G. Müldner, Hs. H. Günthard, W. Gasche, and W. Leuzinger. 1972. The structure of lipids and proteins studied by ATR infrared spectroscopy. I. Oriented layers of tripalmitin. *Z. Naturforsch.* 27b:780–796.
  30. Cornell, B. A. 1981. The effect of the bilayer phase transition on the carbonyl carbon- $^{13}\text{C}$  chemical shift anisotropy. *Chem. Phys. Lipids.* 28:69–78.
  31. Cornell, B. A. 1980. The dynamics of the carbonyl groups in phospholipid bilayers from a study of their  $^{13}\text{C}$  chemical shift anisotropy. *Chem. Phys. Lett.* 72:462–465.
  32. Fraser, R. D. B. 1953. The interpretation of infrared dichroism in fibrous protein structures. *J. Chem. Phys.* 21:1511–1515.
  33. Harrick, N. J. 1967. Internal Reflection Spectroscopy. Interscience Publ., New York.